Anisotropic scale invariance and the uniaxial Lifshitz point from the nonperturbative renormalization group

Gonzalo De Polsi[1, *] and Pawel Jakubczyk[2, †]

[1] *Instituto de Física, Facultad de Ciencias, Universidad de la República, Iguá 4225, Montevideo, Uruguay*

[2] *Institute of Theoretical Physics, Faculty of Physics, University of Warsaw, Pasteura 5, 02-093 Warsaw, Poland*

(Dated: May 11, 2026)

We employ the derivative expansion of the nonperturbative renormalization group to address the phenomenon of anisotropic scale invariance and the associated functional fixed points, also known as Lifshitz points, in systems characterized by a scalar order parameter. We demonstrate the existence of the Lifshitz fixed point featuring a non-classical value of the anisotropy exponent $\theta < 1/2$ and provide estimates for values of a set of critical exponents in the physically most relevant case of the three-dimensional uniaxial Lifshitz point $(d, m) = (3, 1)$, m denoting the anisotropy index. We compare our predictions with existing estimates from perturbative expansions around dimensionality $d = 4 + \frac{1}{2}$ as well as those from the $1/N$ expansion.

I. INTRODUCTION

The phenomenon of scale invariance is amply represented and broadly studied in a diversity of systems of prior relevance to condensed matter and high-energy physics [1–3]. The somewhat less explored and theoretically less understood case concerns anisotropic scale invariance [4–7], where spatial anisotropy of a microscopic system is not smoothened by coarse-graining [8], and achieving scale invariance requires applying the scaling transformation to different directions of the physical space in distinct ways. Such a situation has since long been known to arise in a variety of physical systems including *inter alia* magnets [9–11], liquid crystals [4, 12], polymer systems [7, 13, 14], membranes [15, 16] or quantum chromodynamics [17]. More recently, such setups were also invoked in the contexts of general quantum criticality [18–20], frustrated magnetism [21, 22], altermagnetism [23], unconventional superconductivity [24] and superfluidity of ultra-cold atomic Fermi [25–29] as well as Bose [30–32] gases. For equilibrium condensed matter systems anisotropic scale invariance occurs [4–6], in particular, at the Lifshitz points, i.e. critical points involving three thermodynamic phases, one of them being disordered, one uniformly ordered and the remaining one non-uniformly ordered (i.e. exhibiting modulation of the order parameter). In the standard magnetic setup this corresponds to points in the phase diagram, where paramagnetic, ferromagnetic and antiferromagnetic phases meet. This situation occurs, as already indicated, in ample quantum matter systems being of major present interest. On the other hand, the concept of the Lifshitz point is not at all new and was first discussed already in 1970s [33–36] in relation primarily to magnets. Its most well-studied microscopic realization is presumably in the anisotropic next-nearest-neighbor Ising (ANNNI) model [37]. Despite this long history and the wealth of distinct realizations, description of the Lifshitz points via the renormalization group (RG) tools may be characterized as largely underdeveloped as compared to the isotropic systems. This situation is not hard to explain considering the amount of technical difficulties involved. Notably, the uniaxial Lifshitz point has been perturbatively studied only up to two-loop order [38–40] and the upper critical dimension in question is $d_u = 4 + \frac{1}{2}$, such that extrapolation of the expansion in $\epsilon = d_u - d$ to $d = 3$ is more problematic as compared to the standard isotropic cases, where $d_u^{(isot)} = 4$. Another notable fact is that the Lifshitz exponents have been computed within the $1/N$ expansion only up to terms of order $1/N$ [41, 42] and these two abovementioned approaches, when extrapolated to $(d, N) = (3, 1)$, give conflicting results concerning even the sign of one of the exponents. Relatively recently, the anisotropic Lifshitz point was also addressed in the framework of nonperturbative RG [29, 43]. The latter of these two contributions concentrated exclusively on the case $N = 3$ and used a rather simple and unsystematic approximation, while the former one was restricted to the leading order of the derivative expansion (DE) [the so-called local potential approximation (LPA) or ∂^0] and its minimal extension (referred to as "constrained LPA' "), which mistreated one of the relevant RG eigenpertur-

* gonzalo.depolsi@fcien.edu.uy

† pawel.jakubczyk@fuw.edu.pl

bations. The purpose of the present work is to approach the anisotropic Lifshitz point within the DE retaining all the symmetry-allowed terms at order ∂^2 as well as the physically most relevant terms [44] of order ∂^4, which provides a more systematic and controlled framework. We stress that, in contrast to the standard isotropic situations, inclusion of the ∂^4 term is mandatory due to the physical nature of the problem.

The outline of the present paper is as follows: in Sec. II we introduce and review the analyzed Landau-Ginzburg type model, in Sec. III we discuss an adaptation of the derivative expansion of the nonperturbative RG to anisotropic situations and explain how our equations lead to anisotropic scaling solutions. In Sec. IV we analyze the structure of the flow equations at LPA level, leading to analytical insights and approximate relations with the isotropic setups in reduced dimensionalities, followed by the presentation of our main results concerning the scaling solutions and critical exponents retaining the functional RG flow of the gradient and laplacian terms in the effective action. We summarize the paper in Sec. V.

II. THE LANDAU-GINZBURG MODEL AND ANISOTROPIC SCALE INVARIANCE

We discuss the anisotropic scale invariance in the framework of the Landau-Ginzburg model defined by the bare action [4, 6, 7]:

$$S[\phi] = \int d^d x \left[U^0(\phi^2) + \frac{1}{2}(\nabla_\perp \phi)^2 + \frac{1}{2} Z^0_\parallel (\nabla_\parallel \phi)^2 + \frac{1}{2} W^0_\parallel (\Delta_\parallel \phi)^2 \right] , \tag{1}$$

where ϕ is a real scalar order parameter, and the spatial coordinates involve two classes of components such that

$$d^d x = d^m x_\parallel d^{d-m} x_\perp , \tag{2}$$

$$(\nabla_\parallel \phi)^2 = \sum_{\alpha=1}^{m} \left(\frac{\partial \phi}{\partial x_\alpha} \right)^2 , \quad (\nabla_\perp \phi)^2 = \sum_{\alpha=m+1}^{d} \left(\frac{\partial \phi}{\partial x_\alpha} \right)^2 , \tag{3}$$

and $m \in \{0, 1, \dots d\}$ is the anisotropy index. In the magnetic language, the m distinct space directions represent the ones, to which the possible modulation of the order parameter is constrained. Our major focus is the uniaxial case $m = 1$, however, at formal level, we allow m as well as d to vary continuously. The effective potential $U^0(\phi^2)$ takes the standard form of a quartic polynomial in ϕ:

$$U^0(\phi^2) = \tau \phi^2 + u \phi^4 \tag{4}$$

with $u > 0$. We assume $W^0_\parallel > 0$ and the field ϕ has been defined such that the coefficient of $(\nabla_\perp \phi)^2$ in Eq. (1) is $1/2$.

For $Z^0_\parallel > 0$, as far as universal bulk properties are concerned, there is no essential difference between the two classes of spatial directions and, at mean-field (MF) level, the Laplacian term $W^0_\parallel (\Delta_\parallel \phi)^2$ can be completely disregarded. By varying τ the system is then tuned through a phase transition of ferromagnetic type and, in the RG description, the critical singularities are controlled by the standard Wilson-Fisher fixed point. For $Z^0_\parallel < 0$ it is energetically beneficial for the system to create a spatial modulation of the ordering field ϕ and the magnitude of the ordering wavevector follows from the balance between the gradient and laplacian terms in the $\parallel$ direction. By varying τ one then tunes the system through a transition between the paramagnetic and antiferromagnetic phases, which is again controlled by the Wilson-Fisher RG fixed point. A special situation occurs (at MF level) for $Z^0_\parallel = 0$, where, for $\tau = 0$, the system exhibits an anisotropic scale-invariant critical point (the Lifshitz point) [4, 6, 7]. In particular the MF correlation function

$$\langle \phi_{\vec{q}} \phi_{-\vec{q}} \rangle = G(\vec{q}) = G(\vec{q}_\perp, \vec{q}_\parallel) = \frac{1}{Z_\perp \vec{q}^{\,2}_\perp + W^0_\parallel (\vec{q}^{\,2}_\parallel)^2} \tag{5}$$

depends on the direction of momentum $\vec{q}$. In the vicinity of the Lifshitz point there are two correlation length exponents governing the singularity of the correlation lengths, such that

$$\xi_\perp \sim |\tau|^{-\nu_\perp} , \text{ and } \xi_\parallel \sim |\tau|^{-\nu_\parallel} . \tag{6}$$

Once again, at MF level one finds $\nu_\parallel = \frac{1}{2}\nu_\perp = \frac{1}{4}$. Generically, it can be shown that the two exponents obey the scaling relation [6]

$$\nu_\parallel = \frac{2 - \eta_\perp}{4 - \eta_\parallel} \nu_\perp = \theta \nu_\perp , \tag{7}$$

which defines the anisotropy exponent θ. The quantities $\eta_\perp$ and $\eta_\parallel$ are the anomalous dimensions corresponding to the distinct inequivalent spatial directions. At Lifshitz criticality one anticipates

$$G^{-1}(\vec{q}_\perp, 0) \sim |\vec{q}_\perp|^{2-\eta_\perp} \tag{8}$$

and

$$G^{-1}(0, \vec{q}_\parallel) \sim |\vec{q}_\parallel|^{4-\eta_\parallel} \tag{9}$$

for small momenta.

III. NONPERTURBATIVE RG AND THE DERIVATIVE EXPANSION

As emphasized, in spite of the ample realizations of the Lifshitz criticality in condensed-matter systems, the level of development of the RG (or any other) theory of these phenomena, both in the perturbative and nonperturbative versions, is way lower than for the isotropic cases. We now discuss how the nonperturbative RG calculation is carried out.

Our present approach to the Lifshitz point departs from the 1-particle-irreducible variant of the nonperturbative RG relying on the Wetterich equation [45, 46]

$$\partial_k \Gamma_k[\phi] = \frac{1}{2}\mathrm{Tr}\left[\partial_k R_k(\vec{q})\left(\Gamma_k^{(2)}[\phi] + R_k(\vec{q})\right)^{-1}\right] . \quad (10)$$

Here $\Gamma_k[\phi]$ denotes the effective action in presence of a (momentum) cutoff at scale k, $\Gamma_k^{(2)}[\phi]$ is its second (functional) derivative with respect to ϕ, and $R_k(\vec{q})$ represents the cutoff function suppressing propagation of modes with momentum $\vec{q}$ above the cutoff scale k. For $k \to k_{UV}$ the quantity $\Gamma_k[\phi]$ approaches the bare action $S[\phi]$ such as the one given in Eq. (1), while for $k \to 0$ (cutoff removed) we find $\Gamma_k[\phi] \to F[\phi]$, where $F[\phi]$ represents the Gibbs free energy of the statistical-mechanical system defined by $S[\phi]$. The derivative expansion of the Wetterich equation, introduced already in 1990s [46–53], is presently among the most broadly implemented and successful approximations in this framework and its accuracy is, in many canonical cases, comparable to that achieved by Monte Carlo or high-order perturbation theory. The order ∂^n of the DE consists in projecting the flowing functional $\Gamma_k[\phi]$ onto a set of scale-dependent functions retaining only symmetry-allowed terms involving at most n derivatives of ϕ. For example, for the Lifshitz point at order $n = 4$ we have:

$$\begin{aligned}\Gamma_k^{DE4}[\phi] = \int d^d x \Big\{ & U(\rho) + \frac{1}{2}Z_\perp(\rho)(\nabla_\perp\phi)^2 + \frac{1}{2}Z_\parallel(\rho)(\nabla_\parallel\phi)^2 + \frac{1}{2}W_\perp(\rho)(\Delta_\perp\phi)^2 + \frac{1}{2}W_\parallel(\rho)(\Delta_\parallel\phi)^2 + \\ & \frac{1}{2}X_\perp(\rho)\phi(\nabla_\perp\phi)^2(\Delta_\perp\phi) + \frac{1}{2}X_\parallel(\rho)\phi(\nabla_\parallel\phi)^2(\Delta_\parallel\phi) + \frac{1}{2}Y_\perp(\rho)[(\nabla_\perp\phi)^2]^2 + \frac{1}{2}Y_\parallel(\rho)[(\nabla_\parallel\phi)^2]^2 \\ & + \frac{1}{2}W_\angle(\rho)(\Delta_\parallel\phi)(\Delta_\perp\phi) + \frac{1}{2}X_{1,\angle}(\rho)\phi(\nabla_\parallel\phi)^2(\Delta_\perp\phi) + \frac{1}{2}X_{2,\angle}(\rho)\phi(\nabla_\perp\phi)^2(\Delta_\parallel\phi) + \frac{1}{2}Y_\angle(\rho)(\nabla_\parallel\phi)^2(\nabla_\perp\phi)^2 \Big\} . \end{aligned} \quad (11)$$

We suppressed the k-dependence of the parametrizing functions for clarity of notation and introduced $\rho = \phi^2/2$. Note that the Ansatz of Eq. (11) involves no field truncation and encompasses both the isotropic and anisotropic situations. By inserting the derivative expansion Ansatz into the Wetterich equation [Eq. (10)] one obtains the flow of the parametrizing functions. For the standard $O(N)$ models [54–57], the q-state Potts models [58], or frustrated magnets featuring the $O(N) \times O(2)$ symmetry [59], systematic implementation of the DE leads to very accurate results concerning universal critical properties.

In the practical calculations to follow later in this paper, we will drop the functions $X_\perp$, $X_\parallel$, $X_{1,\angle}$, $X_{2,\angle}$, $Y_\perp$, $Y_\parallel$, $Y_\angle$, $W_\angle$ and $W_\perp$ in Eq. (11), but will retain all the remaining field and scale dependencies. In particular, we account for the renormalization of the single fourth order term $W_\parallel(\rho)\vec{q}_\parallel^{\,4}$, which appears already in the bare action. We refer to this approximation as the "DE(2)+$\mathrm{W}_\parallel(\rho)$ truncation". This truncation is largely analogous to the LPA' approximation commonly applied, inter alia, in the context of isotropic $O(N)$ models. In that procedure one adds a single renormalization field constant Z_k as a flowing coupling of the kinetic term. This allows to compute an estimation of η in a framework largely simplified with respect to the DE(2) truncation and constitutes a minimal step beyond LPA, which captures η. As for the present calculation, in a simplified procedure one might consider just a renormalization constant in front of the $(\Delta_\parallel\phi)^2$ term which would allow us to compute θ at this order of approximation. However, we consider instead the full field dependence of the function $W_\parallel$ which includes the aforementioned coupling as well. Note that, as illustrated in the next section, the function $W_\parallel(\rho)$ does not depart significantly from the constant value 1 which also indicates consistency of this truncation. From the physical point of view, fluctuations in the $\perp$ direction are controlled by the gradient term involving $Z_\perp$ and the neglected terms of order $q_\perp^4$ are then small. The functions $X_{\perp/\parallel/i,\angle}$ and $Y_{\perp/\parallel/\angle}$ are involved in the 3- and 4- point functions [$\Gamma^{(3)}$ and $\Gamma^{(4)}$], respectively, and do not occur in the propagator of the full derivative expansion Ansatz (at any order). The term involving $W_\parallel(\rho)$ must be retained for obvious physical reasons (see Sec. II). In essence, our truncation retains all the DE(2) terms and a single DE(4), which is crucial for capturing the anisotropic Lifshitz point. The anticipated accuracy of the results should be compared to that achieved for the O(N) models at order DE(2). Obtaining the Lifshitz point via the RG flow from a given microscopic action requires tuning two parameters of the bare action, such that the order parameter mass, as well as the gradient coefficient $Z_\parallel$ both vanish in the limit $k \to 0$. In consequence, we anticipate two relevant RG directions at the Lifshitz fixed point. Although we will concentrate on the flow of the Ansatz functions as the scale k of the regulator is varied, we stress that the practical implementation will not consist in fine-tuning two parameters (which is technically quite problematic), but instead will concentrate on finding the fixed point solutions of the dimensionless flow equations starting from a suitable initial guess.

We now focus on the flow of the effective potential $U(\rho)$, which is obtained by first computing $\Gamma^{(2)}$ from

the derivative expansion Ansatz, then plugging the result into Eq. (10) and evaluating at a spatially uniform field configuration. This leads to

$$\partial_k U(\rho) = \frac{1}{2}\int \frac{d^d q}{(2\pi)^d}\partial_k R_k(\vec{q}) G_0(\vec{q},\rho) \tag{12}$$

with

$$\begin{aligned} G_0^{-1}(\vec{q},\rho) &= \\ U'(\rho) &+ 2\rho U''(\rho) + Z_\perp(\rho)\vec{q}_\perp^{\,2} + Z_\parallel(\rho)\vec{q}_\parallel^{\,2} + W_\parallel(\rho)\vec{q}_\parallel^{\,4} + R_k(\vec{q}) \end{aligned} \tag{13}$$

Eq. (12) holds at any order of the DE up to adding [in Eq.(13)] the terms with $W_\angle$, $W_\perp$ (which we disregard here) and terms involving higher powers of momenta in G_0. In Eq. (13) we give the expression pertinent to the DE(2)+W$_\parallel(\rho)$ truncation studied in Sec. IV, i.e. the neglected terms are of order $\vec{q}_\parallel^{\,2}\vec{q}_\perp^{\,2}$, $\vec{q}_\perp^{\,4}$ and $\vec{q}_\parallel^{\,6}$.

In order to seek for RG fixed point solutions, we perform the following rescaling:

$$\begin{aligned} \vec{q}_\perp &= k\tilde{\vec{q}}_\perp\,, \quad \vec{q}_\parallel = k^\theta \tilde{\vec{q}}_\parallel\,, \quad \rho = Z^{-1}k^{d-2+m(\theta-1)}\tilde{\rho}\,, \\ U &= k^{d+m(\theta-1)}\tilde{u}\,, \quad Z_\perp = Z\tilde{z}_\perp\,, \quad Z_\parallel = Zk^{2(1-\theta)}\tilde{z}_\parallel \\ W_\parallel &= Zk^{2(1-2\theta)}\tilde{w}\,, \quad R = Zk^2 r\,, \end{aligned} \tag{14}$$

which absorbs all the explicit dependencies on k in the flow equations for the parametrizing functions. Note that the anisotropy exponent θ is unspecified and actually represents one of the key quantities we set out to compute; while Z is the (scale-dependent) field rescaling factor.

In terms of the rescaled variables, Eq. (12) becomes:

$$\partial_t \tilde{u} = -\left(d + m(\theta-1)\right)\tilde{u} + \left(\eta_\perp + d + m(\theta-1) - 2\right)\tilde{\rho}\tilde{u}' + \mathcal{V}_{d,m}\int_0^\infty d\tilde{q}_\perp \int_0^\infty d\tilde{q}_\parallel \tilde{q}_\perp^{d-m-1}\tilde{q}_\parallel^{m-1}\frac{(2-\eta_\perp)r - 2\tilde{q}^2\partial_{\tilde{q}_\perp^2}r - 2\theta\tilde{q}_\parallel^2\partial_{\tilde{q}_\parallel^2}r}{\tilde{z}_\perp\tilde{q}_\perp^2 + \tilde{z}_\parallel\tilde{q}_\parallel^2 + \tilde{w}\tilde{q}_\parallel^4 + \tilde{u}' + 2\tilde{\rho}\tilde{u}'' + r}\,, \tag{15}$$

where $t = \ln(k/k_{UV})$, $\eta_\perp = -k\partial_t \ln Z$ is the running anomalous dimension corresponding to the $\perp$ direction, and $\mathcal{V}_{d,m} = \frac{1}{2}\frac{\mathcal{S}^{m-1}\mathcal{S}^{d-m-1}}{(2\pi)^d}$ absorbs constants emerging from doing the angular integrations in the two momentum subspaces (here $\mathcal{S}^D$ is the suface area of a unit D-dimensional sphere). Eq. (15) straightforwardly generalizes to higher order DE truncations simply by adding terms involving higher powers of momentum (in the $\perp$ and $\parallel$ directions) in the denominator on its right-hand side. It is evident that Eq. (15) is not closed and must be supplemented by the flow equations for $\tilde{z}_\perp$, $\tilde{z}_\parallel$, and $\tilde{w}$ (which are functions of both k and $\tilde{\rho}$) - see Sec. IV and supplemental material [60].

We additionally observe, that Eq. (15) contains the standard isotropic case at level DE(2), which is recovered by taking $m = 0$ or $\theta = 1$ and setting $\tilde{w} = 0$.

A substantial simplification due to restoration of isotropy occurs also for $m = d$ (the so-called isotropic Lifshitz point). This case is of interest for relativistic theories in $d \geq 4$ and was addressed with nonperturbative RG in Refs. [61–63]. We will not discuss this situation in the present paper.

We now proceed to Sec. IV, where we summarize the LPA approximation, which closes Eq. (15), and subsequently we analyze the DE(2)+W$_\parallel(\rho)$ truncation.

IV. LIFSHITZ POINT IN THE DE(2)+W$_\parallel(\rho)$ TRUNCATION

In this section we present the results stemming from the nonperturbative RG (data available in [64]) and compare to available results in the literature. To this end, we first discuss the LPA approximation which was previously implemented in Ref. [29] and we highlight the differences and the generalization used for the more reliable DE(2)+W$_\parallel(\rho)$ approximation. Subsequently, we present the results obtained with nonperturbative RG for the anisotropic fixed point with $m = 1$ and we compare to the literature. Lastly, we discuss the error bar estimation procedure.

A. The local potential approximation and moving to higher order

We start by reviewing the LPA (∂^0) truncation, where the flow of momentum dependencies of $\Gamma^{(2)}$ is disregarded. In particular, we impose $\tilde{z}_\parallel = 0$. This closes Eq. (15), which can then be studied numerically.

The LPA approximation neglects the anomalous dimensions and implies $\theta = 1/2$. We invoke the observation of Ref. [29] that by taking the dimensionless cutoff r [compare Eq. (14)] in the following form:

$$r(\tilde{\vec{q}}_\perp, \tilde{\vec{q}}_\parallel) = r(\tilde{\vec{q}}_\perp^{\,2} + \tilde{\vec{q}}_\parallel^{\,4}) \tag{16}$$

and performing a suitable rescaling of $\tilde{\rho}$ and $\tilde{u}$, one maps Eq. (15) to its isotropic counterpart in dimensionality $d_{\text{eff}} = d - \frac{m}{2}$. This result implies that the LPA-level fixed point as well as the critical exponents of the m-axial Lifshitz point in d dimensions coincide with those of the $O(N)$ universality class in dimensionality decreased by $m/2$. Even though this correspondence does not hold beyond LPA for $d - \frac{m}{2} < 4$, it becomes increasingly accurate when approaching the upper critical dimension,

where anomalous dimensions vanish. We note that the isotropic $O(1)$ fixed point features only one relevant direction in contrast to the Lifshitz point, which has two; as a consequence, the LPA-level correspondence must, in fact, be violated below $d = 4 + \frac{1}{2}$ in an exact treatment.

The above insights, borrowed from Ref. [29] inspire our strategy of searching for the anisotropic fixed points at order DE(2)+$W_\parallel(\rho)$ which is adopted in Sec. IV. This relies on the above invoked correspondence and exploits its increasing accuracy upon elevating the system dimensionality towards $d_u = 4 + \frac{m}{2}$.

When lifting the truncation to order DE(2)+$W_\parallel(\rho)$, in order to compute the anisotropic scaling solutions the flow of the effective potential [Eq. (15)] must be supplemented with the flow equations for the parametrizing functions $\tilde{z}_\perp(\tilde{\rho})$, $\tilde{z}_\parallel(\tilde{\rho})$, and $\tilde{w}(\tilde{\rho})$. These are derived by the procedure well described e.g. in Ref. [65] for the isotropic situations. By taking consecutive derivatives of the DE(2)+$W_\parallel(\rho)$ Ansatz and evaluating at uniform field configuration, we obtain the vertex functions $\Gamma^{(2)}$, $\Gamma^{(3)}$, $\Gamma^{(4)}$, which depend on ρ and momenta. Subsequently, by differentiating Eq. (10) twice with respect to ϕ we obtain the flow equation for the 2-point function $\Gamma^{(2)}(p_\perp^2, p_\parallel^2, \rho)$, which involves $\Gamma^{(3)}$ and $\Gamma^{(4)}$. In the next step we expand in $p_\perp^2$ and $p_\parallel^2$ and identify the coefficients of the expansion proportional to $p_\perp^2$, $p_\parallel^2$, and $p_\parallel^4$ as flow equations for $Z_\perp(\rho)$, $Z_\parallel(\rho)$, and $W_\parallel(\rho)$, respectively. After performing the rescaling dictated by Eq. (14), we obtain the flow equations characterized by the following structure:

$$\begin{aligned}
\partial_t \tilde{z}_\perp &= \eta_\perp \tilde{z}_\perp + (\eta_\perp + d - 2 + m(\theta-1))\,\tilde{\rho}\tilde{z}'_\perp + \mathrm{L}_{\tilde{z}_\perp} \\
\partial_t \tilde{z}_\parallel &= (\eta_\perp - 2(1-\theta))\,\tilde{z}_\parallel + (\eta_\perp + d - 2 + m(\theta-1))\,\tilde{\rho}\tilde{z}'_\parallel + \mathrm{L}_{\tilde{z}_\parallel} \\
\partial_t \tilde{w} &= (\eta_\perp - 2(1-2\theta))\,\tilde{w} + (\eta_\perp + d - 2 + m(\theta-1))\,\tilde{\rho}\tilde{w}' + \mathrm{L}_{\tilde{w}_\parallel}
\end{aligned} \tag{17}$$

The lengthy loop contributions $\mathrm{L}_{\tilde{z}_\perp}$, $\mathrm{L}_{\tilde{z}_\parallel}$, and $\mathrm{L}_{\tilde{w}_\parallel}$ involve two-dimensional momentum integrals and are explicitly given in the supplemental material. From a technical point of view, the necessity of dealing with controlled numerical two-dimensional momentum integrations constitutes the major challenge as compared to the isotropic situations. Note that the previous studies evaded this complication either by regularizing only some of the directions in momentum space [43], or by disregarding the flow of $Z_\parallel(\rho)$ [29]. The exponents $\eta_\perp$ and θ are determined from the normalization condition which fixes the values of $\tilde{z}_\perp(\tilde{\rho}_0) = 1$ and $\tilde{w}(\tilde{\rho}_0) = 1$ at an arbitrary point $\tilde{\rho}_0$.

Two important aspects should be taken into consideration here.

Firstly, while equations such as (15) and (17) admit locally a multi-parameter family of solutions, physically admissible fixed points are selected by imposing global constraints [47, 48]. These include regularity of the solution for all field values, compatibility with the symmetries of the problem, and appropriate asymptotic behavior at large field. The fixed-point problem is therefore not an initial-value problem but a nonlinear boundary-value problem. For a given choice of regulator and truncation, these global conditions select isolated fixed-point solutions, as is standard in functional renormalization group studies employing the derivative expansion.

Secondly, normalization conditions in the functional renormalization group correspond to fixing redundant directions in theory space, i.e. directions generated by infinitesimal redefinitions of fields and coordinates which do not affect physical observables. In the presence of an infrared regulator, exact reparametrization invariance is broken, but deformed zero modes associated with these redundancies persist and may be fixed by convention. At a Lifshitz fixed point, scale invariance is intrinsically anisotropic and involves independent scaling of perpendicular and parallel coordinates. As a consequence, the quadratic part of the effective action contains two independent kinetic operators, associated with perpendicular and parallel fluctuations, which are not related by symmetry. This implies the existence of two independent redundant rescalings: one associated with the normalization of the field and another one associated with the relative normalization of the perpendicular and parallel kinetic terms. It is therefore consistent to impose two normalization conditions at the fixed point, as described in Eq. (14). These conditions fix redundant directions only and do not constrain physical couplings. After fixing redundant directions, the stability matrix at the fixed point identified below exhibits exactly two negative eigenvalues, corresponding to the two physical relevant perturbations of the Lifshitz universality class. This is consistent with general expectations for Lifshitz critical behavior and with the results reported in this work.

Putting by hand $\tilde{w} = 0$ and imposing $\theta = 1$ we restore symmetry between the $\perp$ and $\parallel$ directions and the flow equations then reduce to the isotropic DE(2) case. We, however, presently seek for a completely different class of fixed point solutions of Eq. (17), which, at least for $d \approx d_u = 4 + m/2$, exhibit $\theta \approx 1/2$.

The cutoff characterized by Eq. (16) is not necessarily the most suitable for the present general case, where $\theta \neq 1/2$. In what follows we take

$$r(\vec{\tilde{q}}_\perp, \vec{\tilde{q}}_\parallel) = \alpha r_0(\vec{\tilde{q}}_\perp^2) r_0(\vec{\tilde{q}}_\parallel^4) \tag{18}$$

with α representing a variable parameter (see below). As concerns the form of the function r_0, we investigated three choices: the Wetterich regulator [66]:

$$r_0(x) = r_W(x) = \frac{x}{e^x - 1}\,, \tag{19}$$

the exponential regulator

$$r_0(x) = r_E(x) = e^{-x}\,, \tag{20}$$

and the "θ_3" regulator

$$r_0(x) = r_{\theta_3}(x) = (1-x)^3 \theta(1-x)\,. \tag{21}$$

The status of the exponential regulator $r_E(x)$ is distinct in the present context since it automatically obeys

Eq. (16). The "θ_3" regulator is a smoothened version of the Litim regulator [67], suitable for analysis reaching above the DE(2) truncation level, for a discussion, see [55]. As already mentioned, our cutoff is entirely different from the one used in Ref. [43], which regularized only the $\|$ directions of momentum. The form given by Eq. (18) is by no means mandatory and is motivated by convenience and the MF and LPA structures of the anisotropic propagator. As we show below, the final numerical values obtained with the three cutoff function families are in fact similar and their differences are small when compared to the estimated error due to the truncation.

B. Anisotropic fixed points for $m = 1$

With the aim of finding fixed-point solutions to Eq. (15) and Eq. (17) we discretize the $\tilde{\rho}$ variable (using a grid of 100 points) and map Eqs. (15), (17) onto a system of ordinary integro-differential equations. Up to computing the integrals, the fixed point equation becomes then represented as a large set of algebraic equations, which can be studied with standard numerical tools relying on Newton's method and its generalizations. In practice, instead of Eq. (15) we use its derivative with respect to $\tilde{\rho}$. Details of the numerical procedure are explained in the Appendix, for a thorough discussion of its different aspects in the isotropic case, see [68]. To identify the Lifshitz fixed point in the physically most relevant case $(d, m) = (3, 1)$, we take advantage of the LPA correspondence described in Sec. IV A. We first consider dimensionality $d = 3.5$, where the LPA approximation is relatively accurate, and where the anisotropic Lifshitz point is expected to be close to the standard isotropic $O(N)$ symmetric fixed point in dimensionality $d = 3$. We use the latter and the value $\theta = 1/2$ as the initial condition for finding the $d = 3.5$ Lifshitz point. We subsequently gradually reduce d using the previously computed fixed point as the new initial condition. This stepping is fully analogous to the procedure implemented for the $O(N)$ models e.g. in Refs. [57, 69]. This procedure works because in this approach, the dimensionality enters as a parameter and does not appear manifestly in vectors dimensionality or as a discretization of space. The fixed-point profiles obtained this way at $d = 3$ are plotted in Figs. 1 and 2. The functions $\tilde{u}'(\tilde{\rho})$ and $\tilde{z}_\perp(\tilde{\rho})$ are qualitatively similar to their counterparts studied previously for the isotropic $O(N)$ classes. Interestingly, the function $\tilde{z}_\parallel(\tilde{\rho})$ is negative only for small values of $\tilde{\rho}$.

Having identified the uniaxial Lifshitz fixed point in $d = 3$, for each of the considered families of regulators, we scan the dependence of the exponents $\eta_\perp$ and θ on the cutoff parameter α. Such dependencies would not occur in an exact calculation and appear due to truncation. We implement the principle of minimal sensitivity (PMS) [70] to choose the values of α, where the observables in question are (locally) least sensitive to the choice of α. For a discussion of the methodology of PMS, its relation to

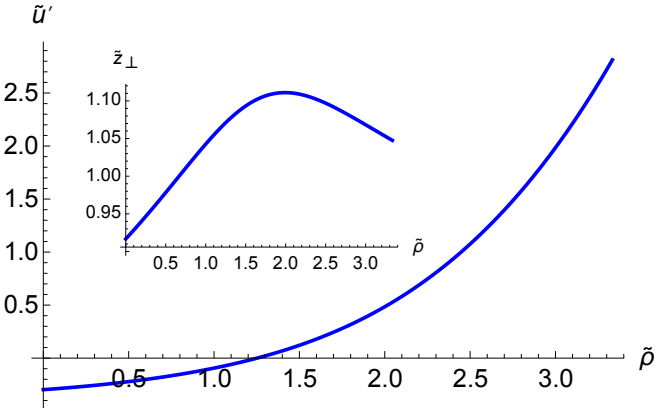

FIG. 1. The derivative of the fixed point effective potential $\tilde{u}'(\tilde{\rho})$ at the uniaxial ($m = 1$) Lifshitz point in $d = 3$. The inset shows the corresponding shape of the function $\tilde{z}_\perp(\tilde{\rho})$. The plot corresponds to the exponential cutoff with $\alpha = \alpha^{(PMS)}_{\eta_\perp} = 0.95$.

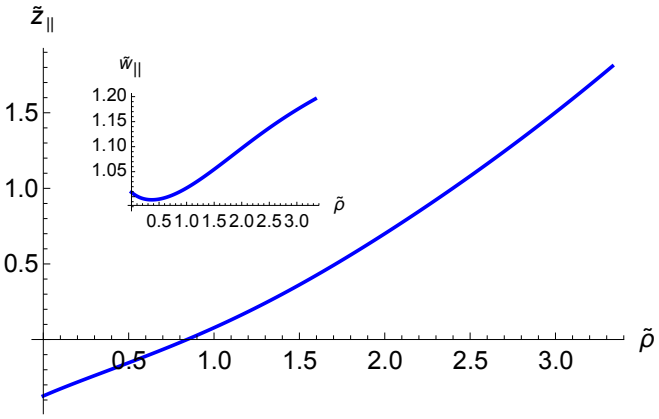

FIG. 2. The fixed point function $\tilde{z}_\parallel(\tilde{\rho})$ at the uniaxial ($m = 1$) Lifshitz point in $d = 3$. The function is negative for small $\tilde{\rho}$. The inset shows the corresponding shape of the function $\tilde{w}_\parallel(\tilde{\rho})$. The plot corresponds to the exponential cutoff with $\alpha = \alpha^{(PMS)}_{\eta_\perp} = 0.95$.

minimal violation of the conformal Ward identity, convergence of the derivative expansion and the nature of its small parameter, see Refs. [54, 71–74]. We present the plots of $\eta_\perp(\alpha)$ and $\theta(\alpha)$ in Figs. 3 and 4. For the final values in $(d, m) = (3, 1)$ we obtain:

$$\theta \approx 0.455\,, \quad \eta_\perp \approx 0.125\,, \quad \eta_\parallel \approx -0.12\,, \tag{22}$$

where, for θ and $\eta_\perp$ we averaged over the PMS values obtained with the three families of regulator. Our value of $\eta_\parallel$ follows from the scaling relation [6]

$$\theta = \frac{2 - \eta_\perp}{4 - \eta_\parallel} \tag{23}$$

already implicit in Eq. (7). For further discussion of the errors and comparison to values obtained from other approaches, see Sec. IV E and Table I.

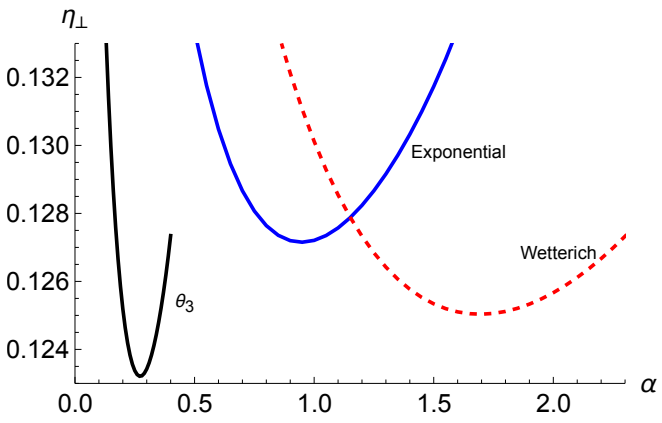

FIG. 3. Dependence of the exponent $\eta_\perp$ on the cutoff parameter α in the DE(2)+W$_\parallel(\rho)$ calculation, plotted for the three considered families of regulators. The PMS value of α as well as the shape of the curve differs substantially depending on the regulator type. However, the PMS value of the exponent differs by the relatively small amount of around 3% depending on the regulator.

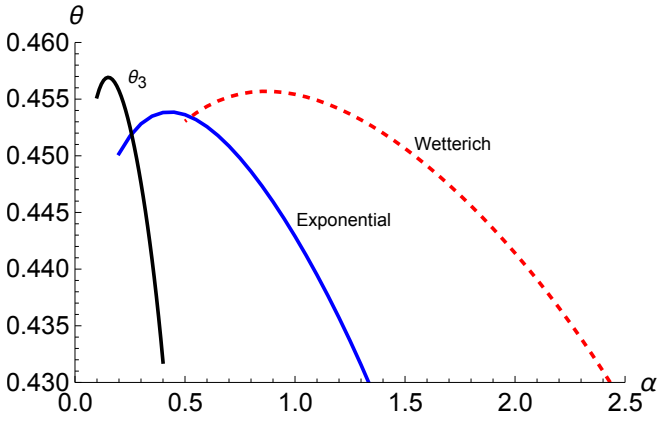

FIG. 4. Dependence of the anisotropy exponent θ on the cutoff parameter α in the DE(2)+W$_\parallel(\rho)$ calculation, plotted for the three considered families of regulators. The PMS value of α as well as the shape of the curve differs substantially depending on the regulator type; the PMS value of the exponent is however almost insensitive with respect to the regulator choice.

We note the negative sign of $\eta_\parallel$, which agrees with predictions of the ϵ-expansion [39] (at order ϵ^2), but not the $1/N$ expansion [40] - compare Table I. We emphasize that accuracy of all these estimates is by no means comparable to the precision reached for the conventional exponents pertinent to the isotropic fixed points, which is reflected by the scatter of the numbers collected in Table I as well as the magnitude of error bars.

As concerns the nonperturbative RG methodology, we believe that the present accuracy of the derivative expansion truncation should be compared to the DE(2) level of the conventional isotropic case. Reaching the complete DE(4) precision is beyond the scope of the present work. We note that the uncertainty estimate of the anomalous dimensions along the lines developed in [54, 55, 71, 72] without elevating the calculation to the complete DE(4) truncation is only possible by using the LPA value $\eta_\perp = \eta_\parallel = 0$. The situation is somewhat different for the correlation length exponents discussed below. We postpone the discussion of errors to Sec. IV E.

C. Correlation lengths and crossover exponents

The values of θ and $\eta_\perp$ follow directly from the fixed-point solution, as described in the preceding section. Further critical exponents can be obtained from the leading eigenvalues of the RG transformation linearized around the fixed point. To construct the latter we introduce the "vector" of parametrizing functions:

$$\mathcal{F}(\tilde{\rho}) := \{\tilde{u}(\tilde{\rho}), \tilde{z}_\perp(\tilde{\rho}), \tilde{z}_\parallel(\tilde{\rho}), \tilde{w}_\parallel(\tilde{\rho})\} \tag{24}$$

and define the stability matrix

$$\mathcal{M}_{(i,\tilde{\rho}_1),(j,\tilde{\rho}_2)} := \left.\frac{\partial\big(\partial_t \mathcal{F}_i(\tilde{\rho}_1)\big)}{\partial \mathcal{F}_j(\tilde{\rho}_2)}\right|_{\eta_\perp^*,\theta^*,\mathcal{F}^*}, \tag{25}$$

where $\mathcal{F}^*$ is the vector of fixed-point functions. This represents the variant of the flow equations linearized around $\mathcal{F}^*$. After discretizing the field $\tilde{\rho}$, we extract the eigenvalues of thus obtained stability matrix.

In accordance with expectations, our calculation always yields two negative eigenvalues (denoted hereafter as e_1 and e_2) corresponding to the two relevant eigenperturbations. We identify the $\nu_\perp$ exponent as $\nu_\perp = e_1^{-1}$ and the crossover exponent ϕ [2, 6] as $\phi = e_2/e_1$. We perform the scan of α dependencies of these two quantities in a procedure analogous to the one implemented for $\eta_\perp$ and θ in Sec.IV B - see Figs. 5 and 6. For the PMS values averaged over the three implemented cutoffs, we find:

$$\nu_\perp \approx 0.679\,, \quad \phi \approx 0.48\,, \quad \nu_\parallel \approx 0.3091\,, \tag{26}$$

where the value of $\nu_\parallel$; follows from $\nu_\parallel = \theta\nu_\perp$ using PMS values of θ and $\nu_\perp$.

D. Discussion

Our final estimates for the critical exponents at the uniaxial Lifshitz point in $d = 3$ are collected and compared to those obtained from other approaches in Table I. We note that none of the previous approaches provide estimates of their errors and therefore the agreement may

	θ	$\eta_\perp$	$\nu_\perp$	$\eta_\parallel$	$\nu_\parallel$	ϕ
MF	1/2	0	1/2	0	1/4	1/2
$O(\epsilon)$ [39]	1/2	0	0.625	0	0.313	0.625
$O(\epsilon^2)$ [39]	0.47	0.039	0.709	-0.019	0.348	0.677
Improved $O(\epsilon^2)$ [40]	0.47	0.124	0.746	-0.019	0.348	0.715
1/N [41, 75]	0.451	0.306	0.726	0.223	0.266	-
LPA (Ref. [29])	1/2	0	0.63	0	-	-
DE(2)+W$_\parallel(\rho)$	**0.455±0.011**	**0.125±0.031**	**0.679±0.012**	**-0.12±0.03**	**0.3091± 0.0093**	**0.48±0.12**

TABLE I. Comparison of the critical exponents controlling the uniaxial Lifshitz point in $d = 3$ obtained from the DE(2)+W$_\parallel(\rho)$ truncation and from other theoretical approaches - the ϵ-expansion around $d = 4 + \frac{1}{2}$ and the $1/N$ expansion, see the main text in Sec. IV C for discussion.

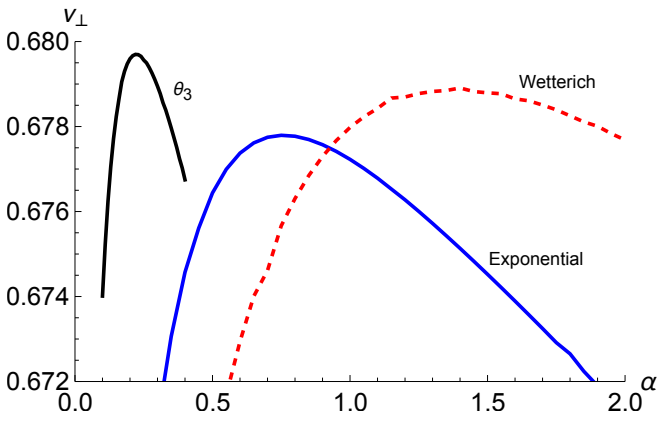

FIG. 5. Dependence of the $\nu_\perp$ exponent on the cutoff parameter α in the DE(2)+W$_\parallel(\rho)$ calculation, plotted for the three considered families of regulators. The PMS value of α as well as the shape of the curve differs substantially depending on the regulator type; the PMS value of the exponent is however almost insensitive with respect to the regulator choice, the difference being of order 0.3% of the value of $\nu_\perp$.

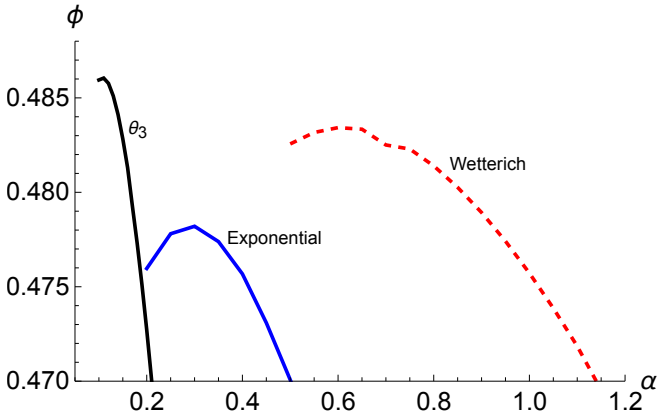

FIG. 6. Dependence of the crossover exponent ϕ on the cutoff parameter α in the DE(2)+W$_\parallel(\rho)$ calculation, plotted for the three considered families of regulators. The PMS value of α as well as the shape of the curve differs substantially depending on the regulator type; the PMS value of the exponent differs by less than 2% of the value of ϕ.

be discussed only at a qualitative level. As a general qualitative observation, we note that for the majority of cases our numbers compare relatively favorably with those of the ϵ-expansion and are often completely off from those from the $1/N$ expansion - see Table I. As concerns the value of θ, there is apparent agreement between all the discussed approaches indicating estimates in the range 0.45-0.47, somewhat below the classical value 1/2. The value 0.47 from the ϵ expansion is nonetheless slightly outside our error bar. For $\eta_\perp$ our result is (presumably by coincidence) very close to one of the predictions from the ϵ-expansion in its resummed variant of Ref. [40] and differs from the one from the $1/N$ approach by a factor larger than 2. Note that the discrepancy between the predictions of the raw (Ref. [39]) and resummed (Ref. [40]) variants of the ϵ expansion exceeds the level of 300% .

The values of $\nu_\perp$ predicted by the three approaches compare well at a qualitative level, however all of the previous results are way outside our uncertainty. For example, the difference between our prediction for $\nu_\perp$ and that of the "improved" ϵ expansion is larger than five times our error. We note that our uncertainty for this exponent reaches below 2% and is significantly lower than for some of the other critical indices (see also Sec. IV E). For $\eta_\parallel$ we obtain a negative value around six times lower than the one from the ϵ expansion (but at least of the same sign). All the earlier results for $\eta_\parallel$ are way outside our error bars and there is no sign of agreement between any of the discussed predictions. This is despite the fact that our error for this quantity reaches the relatively high range of 25%.

In contrast, for $\nu_\parallel$ and ϕ the quoted numbers are in a qualitatively comparable range, even though, again, the previous values are outside our error bar estimates.

As demonstrated in Ref. [29], our method fully recovers the anticipated results in the perturbative regime $d \approx 4 + \frac{1}{2}$, where the ϵ expansion is controlled. We attribute the present disagreements to questionable quantitative reliability of the perturbative techniques, which, for the Lifshitz point, were implemented at relatively low order and extrapolated beyond their range of controllable applicability (where $\epsilon = \frac{3}{2}$).

E. Error estimates

Our error bar estimate methodology is based on the insights of Refs. [54–56, 71], which identify a small parameter of the DE and propose, as well as test, a procedure relying on comparison of results obtained at two consecutive orders of the systematic DE. Within this framework, the error of a quantity κ obtained at order ∂^n of the DE is conservatively estimated as

$$\Delta\kappa^{(n)} = \frac{1}{4}|\kappa^{(n)} - \kappa^{(n-2)}| \,. \tag{27}$$

As we previously emphasized, the analysis of Sec. IV B and IV C should be understood as remaining at the level of DE(2), such that $n = 2$ and $\kappa^{(n-2)}$ corresponds to the LPA prediction, where the anomalous dimensions are absent. In the present situation, this leads to rather large (25%) relative error bars for $\eta_\perp$ and $\eta_\parallel$. The same concerns the crossover exponent ϕ, since LPA suppresses one of the relevant eigendirections related to the gradient term $Z_\perp$, and we adopt $e_2^{(LPA)} = 0$ as the second relevant RG eigenvalue at LPA level. This situation stands in contrast to the other exponents ($\nu_\perp$ in particular), where the relative errors are significantly smaller and reach the accuracy of around 2.4% for θ, 1.8% for $\nu_\perp$ and 3% for $\nu_\parallel$ - see Table I. We also note that the estimated uncertainties from truncation are higher as compared to the one anticipated from the scatter of the PMS values obtained with the three regulator families - See Sec. IV B and IV C.

V. SUMMARY AND OUTLOOK

In recent years the nonperturbative RG methodology has been developed to become a computational tool capable of delivering *inter alia* high-precision numerical estimates of universal critical quantities. It has been extensively tested for the isotropic $O(N)$ models, where predictions from other methods are amply available. In the present study, we adapted and implemented the approach to a far more demanding and nonperturbative situation involving anisotropic scale invariance. In this physical situation no results from high-order perturbation theory or conformal theory are available, and the expansion around the upper critical dimension appears more questionable. In consequence, the values of critical indices cannot be classified as well established up to now. Working directly in $d = 3$, we identified the functional RG fixed point controlling the uniaxial Lifshitz critical behavior and extracted a related set of critical exponents. We emphasize that a highly precise evaluation of these, in particular controlling the error bars, remains an open (and rather long-standing) problem, which in our opinion is partially resolved in the present study only for θ, $\nu_\perp$, and $\nu_\parallel$. On the other hand, in contrast to other techniques, our method provides uncertainty estimates and is quantitatively reliable in the physical dimensionality $d = 3$.

Our results unequivocally confirm the existence of the non-classical Lifshitz point in $d = 3$ with the anisotropy index $\theta \approx 0.46$; a value apparently not far from the predictions from the ϵ-expansion around the upper critical dimension $d = 4 + \frac{1}{2}$ ($\theta \approx 0.47$), and indicate that the deviation from the MF prediction $\theta = 1/2$ is actually not dramatic. Our prediction for the correlation length exponents (in particular for $\nu_\perp$) also compares reasonably with those of the ϵ-expansion (notably the agreement is better with the "raw" variant of the ϵ expansion). In all the cases we consider our estimates to be more reliable than the previous predictions, in particular, with regards to those cases where we are able to provide relatively narrow error bars ($\theta, \nu_\perp, \nu_\parallel$).

Concerning the anomalous dimensions, we find qualitative agreement of $\eta_\perp$ with the ϵ-expansion (in this case the agreement is better with the resummed version of the ϵ expansion). We nevertheless attribute this agreement to a pure coincidence, since the predictions from different variants of the ϵ expansion display huge differences. For $\eta_\parallel$ we disagree with the $1/N$-expansion on both the sign and order of magnitude; while we agree with the ϵ expansion on the sign, but differ on the value by a factor of around 6. Concerning the signs, we also agree with the earlier, simplified and less controlled studies from nonperturbative RG.

Despite certain qualitative agreements we emphasize that, when uncertainties are inspected, most of the predictions of the perturbative methods turn out to fall far outside our error bars. In the particular case of $\eta_\parallel$, where our error estimate is 25%, our prediction differs from the perturbative estimate by a factor larger than 6. This classifies as a rather fatal disagreement and motivates revision of the problem from the perturbation theory point of view and potentially also numerical approaches.

In our opinion going beyond the present truncation level and reaching the precision of the DE(4) approximation is a demanding, but viable enterprise, which would deliver much narrower error estimates of all the critical exponents in question. The same is true concerning an extension to arbitrary values of d and m, except at the vicinity of the lower critical dimension. We are somewhat more reserved about generalization to arbitrary values of N, where going beyond the DE(2)+W$_\parallel(\rho)$ truncation in a controlled fashion represents a formidable challenge.

ACKNOWLEDGMENTS

P.J. acknowledges support from the Polish National Science Center via grant 2021/43/B/ST3/01223 and thanks Ivan Balog for discussions at the initial stage of the project. G.D.P. acknowledges support from the Programa de Desarrollo de las Ciencias Básicas (PEDECIBA) and from the grant of number FCE-3-2024-1-180709 of the Agencia Nacional de Investigación

e Innovación (Uruguay). We are grateful to Nicolas Wschebor for useful remarks on the initial version of the manuscript as well as numerous discussions on related topics. We are indebted to Hans Werner Diehl and Mykola Shpot for a very helpful correspondence.

APPENDIX: NUMERICAL METHOD

We describe in this section the details of the numerical implementation used to find the fixed point and compute the universal critical quantities. The starting point are the flow equations for the different ansatz functions obtained by means of the DE procedure and given in the supplemental material. To treat these expressions numerically there are two key steps: i) Evaluating the flow expressions which involve partial derivatives in the field and internal momenta integration in two independent variables and ii) finding the fixed point solution from a starting initial guess and computing critical quantities of interest from the fixed point solution.

1. Evaluating flow expressions

The expressions to be evaluated involve partial derivatives of the functions in the field. To proceed we consider a uniform grid in the variable ρ with $N_\rho = 101$ points and with a step $\delta\rho = 1/30$. The derivatives are then discretized in the grid with $2m+1$ points centered at each point, except at the m points closest to the each edge where the discretized derivatives are taken as centered as possible.

The flow equations for the ansatz functions involve up to two derivatives which implies that at least three-point derivatives are needed. In the final implementation we used five-point derivatives since results are already stable and considering seven or nine-points derivatives does not alter the results presented here.

Another key aspect of the numerical procedure is the evaluation of the momenta integrals such as the one appearing in Eq.(15) or the ones in the supplemental material. A generic integral $I(\rho)$ appearing in the equations is of the form:

$$I(\rho) = \mathcal{V}_{d,m} \int_0^\infty \int_0^\infty d\tilde{q}_\perp d\tilde{q}_\parallel \tilde{q}_\perp^{d-m-1} \tilde{q}_\parallel^{m-1} f(\tilde{q}_\perp^2, \tilde{q}_\parallel^2, \rho), \tag{28}$$

where f is a function suppressed at large $\tilde{q}_\perp$ or $\tilde{q}_\parallel$ due to the regulator and $\mathcal{V}_{d,m}$ is set to 1 since it can be absorbed in a redefinition of the field and the ansatz functions. The integrals are performed using the Cuhre algorithm of degree 13 from the Cuba library [76]. The upper bound of the integrals were set as $\tilde{q}_\perp^{max} = 3.2$ and $\tilde{q}_\parallel^{max} = 1.8$. Absolute and relative error were chosen to $\varepsilon^{abs} = \varepsilon^{rel} = 10^{-4}$ which yielded same results as higher precision but with a better performance time-wise. Since the Wetterich regulator is ill-defined numerically at 0 momenta, a Taylor expansion up to $o(\tilde{q}_\perp^{P_\perp})$ and $o(\tilde{q}_\parallel^{P_\parallel})$ was considered for momentum $\tilde{q}_\perp \leq Q_\perp^{th}$ and $\tilde{q}_\parallel \leq Q_\parallel^{th}$. We fixed $Q_\perp^{th} = Q_\parallel^{th} = 0.2$ just to be far from numerical instability while having stable integrals. Additionally, the power considered for the Taylor expansion was set to $P_\perp = P_\parallel = 8$ although numerical convergence was obtained for smaller powers of the momenta.

2. Solving for the fixed point and computing critical exponents

As mentioned in the text, to find the fixed point for the Lifshitz model we used as an initial condition the fixed point for the isotropic case in reduced dimensionality. We then proceed to slowly reduce the dimension of the Lifshitz system from dimension $d = 3.5$ to $d = 3$. Subsequently, we proceeded to vary the overall scale of the regulator α.

In order to find a particular fixed point from an initial condition, we performed a straightforward Newton-Raphson (NR) method computing the stability matrix numerically and imposing that β-functions or flows should be negligible enough in order to guarantee for stable results. This, in general, was implemented by imposing a measure of distance and iterating until the norm of the β-function vector $\vec{\beta} \equiv (\beta_{U_0'}, \beta_{U_1'}, \ldots, \beta_{W_{a\parallel,N_\rho-1}})$ was smaller than a threshold ϵ^{dist}.

The fixed-point functions $Z_\perp$ and $W_{a\parallel}$ were normalized as $Z_\perp|_{\rho_{norm}} = W_{a\parallel}|_{\rho_{norm}} = 1$. The normalization point used was $\rho_{norm} = 20\,\delta\rho$. This normalization scheme was implemented throughout the NR procedure which allowed to compute $\eta_\perp$ and θ as a function of the ansatz functions. Once the fixed point was attained, the fixed point critical exponents $\eta_\perp^*$ and θ^* were obtained (see Figs. 3-4).

Once the fixed point is obtained by means of the NR procedure, we perform a linear stability analysis which uses the stability matrix $\mathcal{M}$ already computed in the NR procedure. We then compute the eigenvalues of matrix $\mathcal{M}$ of size $(4N_\rho - 2) \times (4N_\rho - 2)$. There are only two relevant eigenvalues e_1 and e_2 which relate to the correlation length exponent $\nu_\perp$ and to the crossover exponent ϕ as $\nu_\perp = -e_1^{-1}$ and $\phi = e_2/e_1$ (see Figs. 5-6).

In order to find a particular fixed point from an initial condition, we performed a straightforward Newton-Raphson (NR) method computing the stability matrix numerically and imposing that β-functions or flows should be negligible enough in order to guarantee for stable results. This, in general, was implemented by imposing a measure of distance and iterating until the norm of the β-function vector $\vec{\beta} \equiv (\beta_{U_0'}, \beta_{U_1'}, \ldots, \beta_{W_{a\parallel,N_\rho-1}})$ was smaller than a threshold ϵ^{dist}.

We highlight, once again, that all our results were explored by changing parameters (N_ρ, $\delta\rho$, m, $\tilde{q}_\perp^{max}$, $\tilde{q}_\parallel^{max}$,

ε^{abs}, ε^{rel}, ϵ^{dist}, $P_\perp$, $P_\parallel$, $Q_\perp^{th}$ and $Q_\parallel^{th}$) to increase performance and guarantee stability of results.

DATA AVAILABILITY

The numerical data supporting the fixed points and critical exponents are available in the Zenodo repository [64]. The Mathematica notebook containing the derivative expansion ansatz and the derivation of the flow equations is provided as Supplemental Material [60].

[1] N. Goldenfeld, Lect. Phase Transitions Renorm. Gr., 1st ed. (CRC Press, Boca Raton, 1992).
[2] J. Cardy, Scaling and Renormalization in Statistical Physics (Cambridge University Press, 1996).
[3] J. Zinn-Justin, Phase Transitions and Renormalization Group (Oxford University Press, 2007).
[4] P. M. Chaikin and T. C. Lubensky, Princ. Condens. Matter Phys. (Cambridge University Press, Cambridge, 1995).
[5] M. Shpot, Critical behavior of spatially inhomogeneous systems, Ph.D. thesis (2022).
[6] H. W. Diehl, Acta Physica Slovaca **52**, 271 (2002).
[7] R. D. Pisarski, V. V. Skokov, and A. Tsvelik, A pedagogical introduction to the lifshitz regime, Universe **5**, 10.3390/universe5020048 (2019).
[8] X. S. Chen and V. Dohm, Nonuniversal finite-size scaling in anisotropic systems, Phys. Rev. E **70**, 056136 (2004).
[9] C. C. Becerra, Y. Shapira, N. F. Oliveira, and T. S. Chang, Lifshitz point in mnp, Phys. Rev. Lett. **44**, 1692 (1980).
[10] P. Butera and M. Pernici, $(m, d, n) = (1, 3, 2)$ lifshitz point and the three-dimensional xy universality class studied by high-temperature bivariate series for xy models with anisotropic competing interactions, Phys. Rev. B **78**, 054405 (2008).
[11] T. Plackowski, D. Kaczorowski, and J. Sznajd, Magnetic phase diagram and possible lifshitz critical point in upd_2si_2, Phys. Rev. B **83**, 174443 (2011).
[12] J.-h. Chen and T. C. Lubensky, Landau-ginzburg mean-field theory for the nematic to smectic-c and nematic to smectic-a phase transitions, Phys. Rev. A **14**, 1202 (1976).
[13] A. V. Dobrynin and L. Leibler, Theory of random copolymers near the lifshitz point, Europhysics Letters **36**, 283 (1996).
[14] D. Schwahn, K. Mortensen, H. Frielinghaus, and K. Almdal, Crossover from 3d ising to isotropic lifshitz critical behavior in a mixture of a homopolymer blend and diblock copolymer, Phys. Rev. Lett. **82**, 5056 (1999).
[15] L. Radzihovsky and J. Toner, A new phase of tethered membranes: Tubules, Phys. Rev. Lett. **75**, 4752 (1995).
[16] K. Essafi, J.-P. Kownacki, and D. Mouhanna, Crumpled-to-tubule transition in anisotropic polymerized membranes: Beyond the ϵ expansion, Phys. Rev. Lett. **106**, 128102 (2011).
[17] R. Casalbuoni and G. Nardulli, Inhomogeneous superconductivity in condensed matter and qcd, Rev. Mod. Phys. **76**, 263 (2004).
[18] R. Ramazashvili, Quantum lifshitz point, Phys. Rev. B **60**, 7314 (1999).
[19] F. Günther, G. Seibold, and J. Lorenzana, Quantum lifshitz point in the infinite-dimensional hubbard model, Phys. Rev. Lett. **98**, 176404 (2007).
[20] B. Zhao, J. Takahashi, and A. W. Sandvik, Multicritical deconfined quantum criticality and lifshitz point of a helical valence-bond phase, Phys. Rev. Lett. **125**, 257204 (2020).
[21] L. Balents and O. A. Starykh, Quantum lifshitz field theory of a frustrated ferromagnet, Phys. Rev. Lett. **116**, 177201 (2016).
[22] Y. A. Kharkov, J. Oitmaa, and O. P. Sushkov, Quantum lifshitz criticality in a frustrated two-dimensional xy model, Phys. Rev. B **101**, 035114 (2020).
[23] H. Hu and X.-J. Liu, Quantum lifshitz points in an altermagnetic metal (2025), arXiv:2505.10242 [cond-mat.supr-con].
[24] J. Wårdh, B. M. Andersen, and M. Granath, Suppression of superfluid stiffness near a lifshitz-point instability to finite-momentum superconductivity, Phys. Rev. B **98**, 224501 (2018).
[25] K. B. Gubbels, J. E. Baarsma, and H. T. C. Stoof, Lifshitz point in the phase diagram of resonantly interacting ^{6}Li–^{40}**K** mixtures, Phys. Rev. Lett. **103**, 195301 (2009).
[26] D. Pimenov, I. Mandal, F. Piazza, and M. Punk, Non-fermi liquid at the fflo quantum critical point, Phys. Rev. B **98**, 024510 (2018).
[27] P. Zdybel and P. Jakubczyk, Quantum lifshitz points and fluctuation-induced first-order phase transitions in imbalanced fermi mixtures, Phys. Rev. Res. **2**, 033486 (2020).
[28] M. Pini, P. Pieri, and G. Calvanese Strinati, Strong fulde-ferrell larkin-ovchinnikov pairing fluctuations in polarized fermi systems, Phys. Rev. Res. **3**, 043068 (2021).
[29] P. Zdybel, M. Homenda, A. Chlebicki, and P. Jakubczyk, Stability of the fulde-ferrell-larkin-ovchinnikov states in anisotropic systems and critical behavior at thermal m-axial lifshitz points, Phys. Rev. A **104**, 063317 (2021).
[30] P. Jakubczyk and J. Wojtkiewicz, Phase diagram and correlation functions of the anisotropic imperfect bose gas in d dimensions, Journal of Statistical Mechanics: Theory and Experiment **2018**, 053105 (2018).
[31] M. Łebek and P. Jakubczyk, Dimensional crossovers and casimir forces for the bose gas in anisotropic optical lattices, Phys. Rev. A **102**, 013324 (2020).
[32] M. Łebek and P. Jakubczyk, Thermodynamic Casimir forces in strongly anisotropic systems within the $N \to \infty$ class, SciPost Phys. Core **4**, 016 (2021).
[33] R. M. Hornreich, M. Luban, and S. Shtrikman, Critical behavior at the onset of $\vec{k}$-space instability on the λ line, Phys. Rev. Lett. **35**, 1678 (1975).
[34] A. Michelson, Phase diagrams near the lifshitz point. i. uniaxial magnetization, Phys. Rev. B **16**, 577 (1977).
[35] A. Michelson, Phase diagrams near the lifshiftz point. ii. systems with cylindrical, hexagonal, and rhombohedral

symmetry having an easy plane of magnetization, Phys. Rev. B **16**, 585 (1977).
[36] G. S. Grest and J. Sak, Low-temperature renormalization group for the lifshitz point, Phys. Rev. B **17**, 3607 (1978).
[37] W. Selke, The annni model — theoretical analysis and experimental application, Physics Reports **170**, 213 (1988).
[38] C. Mergulhão and C. E. I. Carneiro, Field-theoretic calculation of critical exponents for the lifshitz point, Phys. Rev. B **59**, 13954 (1999).
[39] H. W. Diehl and M. Shpot, Critical behavior at m-axial lifshitz points: Field-theory analysis and ϵ-expansion results, Phys. Rev. B **62**, 12338 (2000).
[40] M. Shpot and H. Diehl, Two-loop renormalization-group analysis of critical behavior at m-axial lifshitz points, Nuclear Physics B **612**, 340 (2001).
[41] M. A. Shpot, Y. M. Pis'mak, and H. W. Diehl, Large-n expansion for m-axial lifshitz points, Journal of Physics: Condensed Matter **17**, S1947 (2005).
[42] M. A. Shpot, H. W. Diehl, and Y. M. Pis'mak, Compatibility of 1/n and ϵ expansions for critical exponents at m-axial lifshitz points, Journal of Physics A: Mathematical and Theoretical **41**, 135003 (2008).
[43] K. Essafi, J.-P. Kownacki, and D. Mouhanna, Nonperturbative renormalization group approach to lifshitz critical behaviour, Europhysics Letters **98**, 51002 (2012).
[44] We emphasize that the phrase *most relevant* is not meant in the technical sense of RG, but rather as a literal expression referring to the terms expected to dominate the physics at the Lifshitz point.
[45] C. Wetterich, Exact evolution equation for the effective potential, Phys. Lett. B **301**, 90 (1993).
[46] T. R. Morris, Derivative expansion of the exact renormalization group, Physics Letters B **329**, 241 (1994).
[47] T. R. Morris, On truncations of the exact renormalization group, Physics Letters B **334**, 355 (1994).
[48] T. R. Morris, The renormalization group and two dimensional multicritical effective scalar field theory, Physics Letters B **345**, 139 (1995).
[49] T. R. Morris, Properties of derivative expansion approximations to the renormalization group, International Journal of Modern Physics B **12**, 1343 (1998).
[50] G. v. Gersdorff and C. Wetterich, Nonperturbative renormalization flow and essential scaling for the kosterlitz-thouless transition, Phys. Rev. B **64**, 054513 (2001).
[51] C. Bagnuls and C. Bervillier, Exact renormalization group equations: an introductory review, Physics Reports **348**, 91 (2001), renormalization group theory in the new millennium. II.
[52] L. Canet, B. Delamotte, D. Mouhanna, and J. Vidal, Nonperturbative renormalization group approach to the ising model: A derivative expansion at order ∂^4, Phys. Rev. B **68**, 064421 (2003).
[53] B. Delamotte, D. Mouhanna, and M. Tissier, Nonperturbative renormalization-group approach to frustrated magnets, Phys. Rev. B **69**, 134413 (2004).
[54] I. Balog, H. Chaté, B. Delamotte, M. Marohnić, and N. Wschebor, Convergence of nonperturbative approximations to the renormalization group, Phys. Rev. Lett. **123**, 240604 (2019).
[55] G. De Polsi, I. Balog, M. Tissier, and N. Wschebor, Precision calculation of critical exponents in the o(n) universality classes with the nonperturbative renormalization group, Phys. Rev. E **101**, 042113 (2020).
[56] G. De Polsi, G. Hernández-Chifflet, and N. Wschebor, Precision calculation of universal amplitude ratios in o(n) universality classes: Derivative expansion results at order $O(\partial^4)$, Phys. Rev. E **104**, 064101 (2021).
[57] A. Chlebicki, C. A. Sánchez-Villalobos, P. Jakubczyk, and N. Wschebor, F_4-symmetric perturbations to the xy model from functional renormalization, Phys. Rev. E **106**, 064135 (2022).
[58] C. A. Sánchez-Villalobos, B. Delamotte, and N. Wschebor, q-state potts model from the nonperturbative renormalization group, Phys. Rev. E **108**, 064120 (2023).
[59] C. A. Sánchez-Villalobos, B. Delamotte, and N. Wschebor, $\mathrm{O}(n) \times \mathrm{O}(2)$ scalar models: Including $o(\partial^2)$ corrections in the functional renormalization group analysis, Phys. Rev. E **111**, 034104 (2025).
[60] See supplemental material at [url] for the explicit derivative expansion ansatz and the derivation of the associated flow equations.
[61] D. Zappalà, Isotropic lifshitz point in the o(n) theory, Physics Letters B **773**, 213 (2017).
[62] D. Zappalà, Indications of isotropic lifshitz points in four dimensions, Phys. Rev. D **98**, 085005 (2018).
[63] N. Defenu, A. Trombettoni, and D. Zappalà, Topological phase transitions in four dimensions, Nuclear Physics B **964**, 115295 (2021).
[64] G. De Polsi and P. Jakubczyk, Dataset for APS manuscript: Anisotropic scale invariance and the uniaxial Lifshitz point from the nonperturbative renormalization group (2026).
[65] N. Dupuis, L. Canet, A. Eichhorn, W. Metzner, J. Pawlowski, M. Tissier, and N. Wschebor, Physics Reports **910**, 1 (2021).
[66] J. Berges, N. Tetradis, and C. Wetterich, Nonperturbative renormalization flow in quantum field theory and statistical physics, Phys. Rep. **363**, 223 (2002), 0005122 [hep-ph].
[67] D. F. Litim, Optimized renormalization group flows, Phys. Rev. D **64**, 105007 (2001).
[68] A. Chlebicki, Numerical accuracy of the derivative-expansion-based functional renormalization group, Journal of Statistical Mechanics: Theory and Experiment **2024**, 093204 (2024).
[69] A. Chlebicki and P. Jakubczyk, Analyticity of critical exponents of the $O(N)$ models from nonperturbative renormalization, SciPost Phys. **10**, 134 (2021).
[70] L. Canet, B. Delamotte, D. Mouhanna, and J. Vidal, Optimization of the derivative expansion in the nonperturbative renormalization group, Phys. Rev. D **67**, 065004 (2003).
[71] I. Balog, G. De Polsi, M. Tissier, and N. Wschebor, Conformal invariance in the nonperturbative renormalization group: A rationale for choosing the regulator, Phys. Rev. E **101**, 062146 (2020).
[72] G. De Polsi and N. Wschebor, Regulator dependence in the functional renormalization group: A quantitative explanation, Phys. Rev. E **106**, 024111 (2022).
[73] B. Delamotte, G. De Polsi, M. Tissier, and N. Wschebor, Conformal invariance and composite operators: A strategy for improving the derivative expansion of the nonperturbative renormalization group, Phys. Rev. E **109**, 064152 (2024).
[74] S. Cabrera, G. De Polsi, and N. Wschebor, Conformal invariance constraints in the $o(n)$ models: A study within the nonperturbative renormalization group, Phys. Rev. E

111, 054126 (2025).
[75] M. Shpot and Y. Pis'mak, Lifshitz-point correlation length exponents from the large-n expansion, Nuclear Physics B **862**, 75 (2012).
[76] T. Hahn, Cuba—a library for multidimensional numerical integration, Computer Physics Communications **168**, 78 (2005).